Online Self-Tuning Power System Stabilizer Based on the Speed Gradient

Mohammed MEKHANET[1] and Lakhdar MOKRANI[2]

[1, 2]Electrical Engineering Department, Amar Telidji University, BP G37 Laghouat, Algeria
[1, 2]LACoSERE Laboratory, Electrical Engineering Department Amar Telidji University of Laghouat, Algeria.
[1]m.mekhanet@lagh-univ.dz , [2]l.mokrani@lagh-univ.dz

Abstract: This work describes an online auto-adjustment of the lead-lag Power System Stabilizer (PSS) parameters. The implemented self-tuning technique adjusts the Conventional Power System Stabilizer (CPSS) gain amplifier or one of its time constants based on generator speed gradient, in order to enhance the stability of Single-Machine Infinite Bus SMIBS and multimachine power systems. The proposed Self-Tuned Power System Stabilizer (STPSS) parameters are updated according to the speed variation (gradient).Therefore it is more robust than the CPSS when subjected to large disturbances. The particularity of this controller is that it varies its damping coefficient in real time according to the variation of its parameters (gain or time constant). On the other hand, this PSS does not vary its parameters in the steady state for a given load, and behaves like a simple CPSS. However, if there is a disturbance, the PSS reacts to create the necessary torque by auto-updating its parameters according to the variation of the speed gradient. Simulations are carried out using the proposed STPSS to show that it consistently gives a stable response with an acceptable overshoots and settling times on speed deviation. The proposed PSS is a good choice among conventional PSSs (easy to implement but under-performing) and other adaptive PSSs (high-performing but very complex).

Keywords: SMIBS, Dynamic Stability; Power System Stabilizer; Self-Tuning; PSS; conventional PSS; Performance comparison.

1. Introduction

The high complexity and nonlinearity of power systems have presented a deal of challenge to power control system engineers for a long time. One of the most important problems in power systems is the damping of low-frequency oscillations, which may grow and lead to a dynamic instability of the system for lower damping torque. In order to overcome this problem and improve the dynamic stability of the power system, the idea of using an additional stabilizing signal to the excitation systems has been largely considered in last two decades [1]. The conventional lead lag PSS was first proposed in the 1960s and classical control theory, described in transfer functions, was performed for its design and applied in power plants. One important issue in this regard is the tuning of the power system stabilizer parameters. To increase the damping of the power system response, classical controllers, which are usually designed for an operating point, can be used. However, the desired PSS should stabilize the power system in a wide range of operating points. In fact, it should be robust against power system variation parameters and the changes in the operation conditions [2-3].

The CPSS remains the most popular design approach used in industrial power system applications due to its simplicity and reliability to attenuate the power oscillations [4]. As it has been mentioned, the basic function of a power system stabilizer is to extend stability limits by modulating generator excitation to provide damping torque to the rotoric oscillations of the synchronous machine. These oscillations of concern typically occur in the frequency range of approximately 0.2 to 2.5 Hz and insufficient damping of these oscillations may limit the transmit power [5-6]. In the literature, different methods have been proposed to suppress the mentioned oscillations in the power system. The PSS has been one of the traditional devices used to damp out these oscillations [3]. A large number of research papers have appeared in the

Received: October 29th, 2018. Accepted: May 7th, 2020
DOI: 10.15676/ijeei.2020.12.2.3

area of PSS design. In 1969, DeMello and Concordia proposed the first PSS [6], but this study concluded that a universally applicable stabilizing function is not practically feasible [7]. The principal problem associated with the PSS is to determine the parameters, because the power system is highly nonlinear and operates in a constantly changing environment (loads, generator outputs, topology, and key operating parameters change continually …) [8].

Various control strategies and optimization techniques have found their applications in this area. In fact, to design a PSS with better performance, several approaches have been applied and many useful results have been published. These include optimal control, adaptive control, variable structure control and different optimization and artificial intelligence techniques [9]. The problem is that this kind of PSS is not easy to implement, even though it is more robust and high-performing than a CPSS. The main problem lies in the PSS proposal that adapts any eventuality. Generally, the PSS design methods can be divided into three categories, [10]:

The methods of linear control are generally based on the analysis of sensitivity to eigenvalues such as pole placement, methods of nonlinear control such as adaptive control, fuzzy logic, and empirical methods of control such as technical artificial intelligence. The basic function of adaptive control is to adjust the parameters in real time and according to the behavior of the available power system and good damping over a wide operating range. All adaptive control techniques can be divided into two different groups, [11]:

- A direct optimal control with optimal parameters calculated off-line for a "reference scenario" and then applied on the system;
- An adaptive optimal control with optimal control laws that are mounted on-line on the real state of the system.

Here is a non-exhaustive state of the art corresponding to the self-tuning PSSs based on adaptive control techniques. In 1990, a PSS using a decentralized self-adjusting control system has been proposed [12]. It has been followed by another work in which the suggested controller adjusts automatically the parameters by minimizing the input integral squares error [13]. Two other articles published in 1994, proposed an experimental study by implementation of a self-adaptive optimized PSS, using the shift method poles [14]. Elsewhere, an adaptive PSS based on an implicit approach, that allows the direct identification of PSS parameters in 1995 [15]. Another approach for setting online the PSS parameters using radial neural networks has been provided in [16], in 1999. In 2004, a systematic approach for the design of a PSS auto-tuning procedure based on Artificial Neural Networks (ANN) also has been presented in [17]. This ANN is used for auto-tuning of PSS parameters in real time. Another model of adaptive power system stabilizer in 2010 [18]. This adaptive PSS consists of a linear element based on an identifier that identifies an average of the power system third order model (Auto-Regressive Moving Average (ARMA)) and a discrete pole-shift displacement controller. Recently, a new stabilizer developed around an adaptive fuzzy sliding mode approach that applies the Nussbaum gain in order to enhance the power system stability in 2013 [19].

In summary, it is noted that there are several types of conventional PSSs (such as lead lag conventional PSS, multi-band PSS, PID PSS ...) characterized by fixed parameters. However, the use of this type of PSSs to well damp rotor oscillations of power systems is not sufficiently effective especially when the operating conditions change, or when there is a major disturbance such as a short circuit [6][20]. Moreover, another category of PSSs, called optimized and adaptive PSSs, are very important for their reliability and adaptation to different operating conditions. Another category to mention is, the conventional PSSs with optimized parameters by meta-heuristics techniques (such as local, global or hybrid optimization research methods) [21]. The negative sides of these techniques is that they require a significant computational time and a large data memory. Since the dynamics and parameters of power systems are nonlinear and vary greatly over time, these PSSs with adaptive parameters, which depend on the operation point, are used to overcome the disadvantage of PSSs with fixed-parameters.

Another kind of PSSs to mention is based on a real-time adaptation of the controller settings by the use of a pre-established database. Artificial intelligence techniques such as neural networks and neuro-fuzzy systems can be used for this purpose [22]. This involves generating a database in a deferred time (using optimization technique) and then using that database as a target for learning these intelligent systems. The main inconvenience of this category of PSSs is that if the system will work outside the learning limits, the generated parameters can be outliers causing the system to malfunction. In addition, the time taken to learn and generate the database is considerable, especially if the case has large number of PSSs. Advanced techniques (such as optimal control, adaptive and/or predictive control …) can also be used to build high-performing and robust PSSs [23-25]. However, this kind of angular stability controllers is more difficult to design and/or implement.

2. Investigated System

The present investigations considers a single machine-infinite bus system. It is constituted of a machine connected to a large power system through a transmission line (see Figure 1).

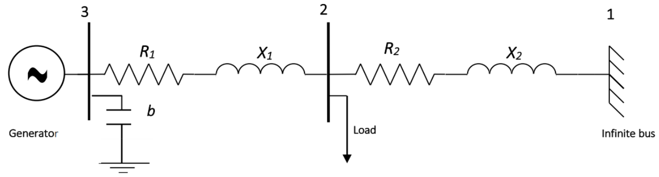

Figure 1. A single machine-infinite-bus power system

Because of the relative size of the system to which the machine is supplying power, the dynamics associated with the machine will cause virtually no change in the voltage and frequency of the infinite bus voltage [25-28].The system parameters are given in the appendix.

3. Power System Model

The SMIBS state-space model can be expressed as follows [7]:

$$\frac{d\underline{X}(t)}{dt} = A\underline{X}(t) + B\underline{U}(t) + \Gamma P(t) \tag{1}$$

With:

$$\underline{X}(t) = \left[\Delta\omega, \Delta\delta, \Delta E_q^{'}, \Delta E_{fd}\right]^T \tag{2}$$

Where, *X(t)*, *U(t)* and *P(t)* are the state variables, the control and the disturbance vectors respectively. In addition, the matrices A, B and *r* are given by:

$$A = \begin{bmatrix} \frac{-D}{2H} & \frac{-K_1}{2H} & \frac{-K_2}{2H} & 0 \\ 2\pi f & 0 & 0 & 0 \\ 0 & \frac{-K_3}{T_{d0}^{'}} & \frac{-K_4}{T_{d0}^{'}} & \frac{-1}{T_{d0}^{'}} \\ 0 & \frac{-K_aK_5}{T_a} & \frac{-K_aK_6}{T_a} & \frac{-1}{T_a} \end{bmatrix} \tag{3}$$

$$B = \begin{bmatrix} 0 & 0 & 0 & \frac{K_a}{T_a} \end{bmatrix} \tag{4}$$

$$\Gamma = \begin{bmatrix} \frac{1}{2H} & 0 & 0 & 0 \end{bmatrix} \tag{5}$$

The constants K_i=1 …6 which depend on the system data are defined as follow [7]:

$K_1 = \frac{\partial P_e}{\partial \delta}$, $K_2 = \frac{\partial P_e}{\partial E_q^{'}}$, $K_3 = \frac{\partial E_q}{\partial E_q^{'}}$, $K_4 = \frac{\partial E_q}{\partial \delta}$, $K_5 = \frac{\partial V}{\partial \delta}$ and $K_6 = \frac{\partial V}{\partial E_q^{'}}$, See Table 9 (Appendix) for symbols meaning.

The SMIBS block diagram is given in the following figure:

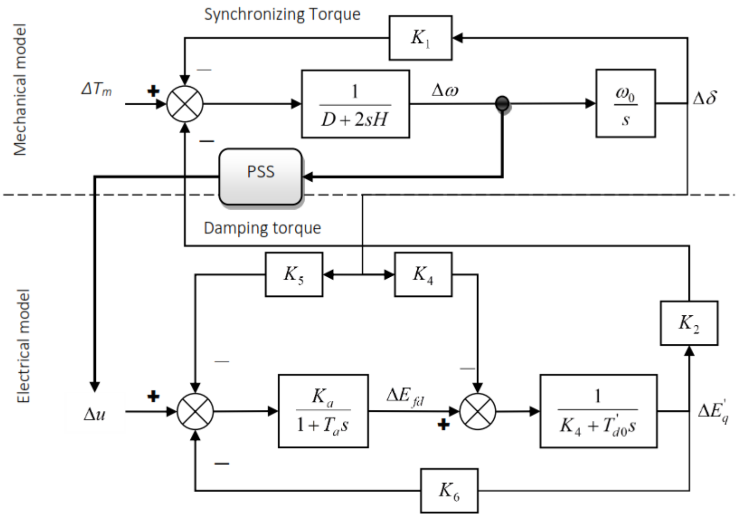

Figure 2. Block diagram of a SMIBS equipped with a PSS

4. Conventional Lead Lag PSS

The PSS is an additional control system that is often applied as a part of an excitation control system. The basic function of the PSS is to apply an additive signal to the excitation system in order to produce an electrical torque in phase with speed deviation that damps out the rotoric oscillations. It performs within the generator's excitation system to create a part of electrical torque, called damping torque, proportional to the speed change. Since the 1960s, PSSs have been used to enhance the damping of the electromechanical oscillations. Later in 1969, a revolutionary work has exhibited great interest and made significant assistance in PSS design and applications for both single and multimachine power systems [27]. The PSS considered here is formed by an amplifier gain K_c, a conventional lead-lag blocks network (with lead lag time constants $T_{1,3}$ and $T_{2,4}$ respectively) and a washout circuit of a time constant, see figure 3[20], [29-32]. The washout block acts as a high-pass filter that allows the signal associated with the oscillations in rotor speed to pass unchanged. Furthermore, it does not allow the steady state changes to modify the terminal voltage. The phase compensation blocks supply the suitable phase-lead characteristics to compensate the phase lag between the input and the output signals [28].

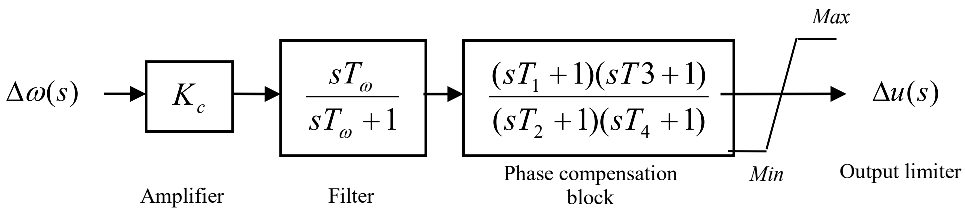

Figure 3. Block diagram of a lead-lag phase PSS

The transfer function of this lead-lag PSS is given by:

$$\frac{\Delta u(s)}{\Delta\omega(s)} = K_c\left(\frac{sT_\omega}{1+sT_\omega}\right)\left(\frac{1+sT_1}{1+sT_2}\right)\left(\frac{1+sT_3}{1+sT_4}\right) \tag{6}$$

We can choose $T_1=T_3$ and $T_2=T_4$ for simplicity reason. The Washout filter permits to block the unwanted frequencies below 0.1 Hz. Its time constant (T_ω) is not very critical since it is generally taken between 1s and 20s. In this study, it is set to 10s.

Generally, conventional power system stabilizers are designed based on the linearized theory in order to well damp out the rotoric oscillations for a particular operating point. For this purpose, an eigenvalue analysis is usually used as a basic tuning technique to compensate for the phase lags by providing a damping torque component. Consequently, since power systems are nonlinear, CPSSs are not effective systematically for a wide range of operating conditions [33-36].

5. A Novel Self-Tuning PSS

The proposed PSS adjusts online the parameters, K_c ,T_1 or T_2 for each sampling time on the basis of the speed gradient $\frac{\partial(\Delta\omega)}{\partial K_c}, \frac{\partial(\Delta\omega)}{\partial T_1}$ or $\frac{\partial(\Delta\omega)}{\partial T_2}$ in order to well damp the rotoric oscillations of the power system generator (see Figure 4).

The choice of the parameter to tune in this manner depends on the speed sensitivity to these three parameters. Consequently, because of the speed variation relatively to each parameter and the sensitivity analysis, one of the PSS three parameters will be tuned online.

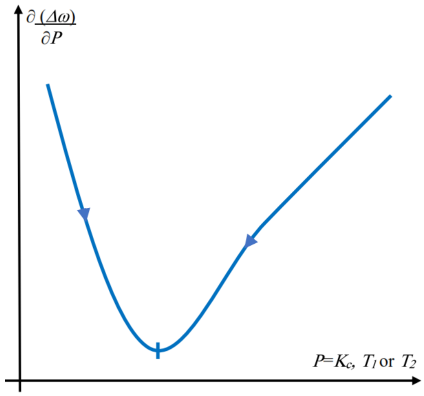

Figure 4. Principle of the PSS parameter adjustment

Hence, starting from the parameters of a PSS globally optimized by the genetic algorithm, the proposed procedure updates online the parameters using the following equations:

$$K_C(k+1) = K_C(k) - \alpha\left(\frac{\partial(\Delta\omega)}{dK_C}\right) \tag{7}$$

$$T_1(k+1) = T_1(k) - \beta\left(\frac{\partial(\Delta\omega)}{dT_1}\right) \tag{8}$$

$$T_2(k+1) = T_2(k) - \gamma\left(\frac{\partial(\Delta\omega)}{dT_2}\right) \tag{9}$$

Practically, this self-tuning procedure is carried out as follows:

- Determination of optimal basic parameters ($K_c^{'}, T_1^{'}$ and $T_2^{'}$) using an eigenvalue analysis and genetic algorithm;
- Analysis of the speed oscillations sensitivity around the PSS three parameters optimal values;
- Setting the variation ranges of each parameter;

- The optimization of the coefficients (*α, β* or *γ*) to be used to tune the PSS parameter. To determine these parameters, one can minimize the speed deviation ISE (Integral Squared error).

6. Design of the Proposed PSS

A. Sensitivity analysis

The sensitivity analysis is a useful method to test the adequacy of varying a given PSS parameter in terms of rotoric oscillations damping. In this case, this sensitivity analysis is performed for the closed-loop power system.

The performance index has been chosen as the speed Integral Squared Error (ISE):

$$ISE = \int_{t=0}^{t_f} \Delta\omega^2 dt \qquad (10)$$

Where t_f is the simulation time.

The speed dynamic error (or derivation) has been calculated in the case of a three-phase short circuit fault of 100 ms that occurs at t=1s applied to the node number 2 of the SMIBS.

To determine this sensitivity index, the parameters were globally optimized by the genetic algorithm based on an eigenvalue analysis in a first step [29]. The obtained values are the following: $K_c^{'}$ =40; $T_1^{'} = T_3^{'}$=0.20s and $T_2^{'} = T_4^{'}$=0.078s.

Let us now determine the speed sensitivity to these three key parameters K_C, T_1 and T_2, by varying them around their optimal values. Table 1 summarizes the obtained results:

Table 1. Speed sensitivity to K_c, T_1 and T_2 variation

Case of K_C variation							
ΔK_C	-70%	-30%	-10%	0%	10%	50%	70%
ΔISE (%)	-40.30	-10.31	-1,72	0	0.22	16,17	75.65
Case of T_1 variation							
ΔT_1	-70%	-30%	-10%	0%	10%	50%	70%
ΔISE(%)	-35.30	-4.67	-1.83	0	1.67	15.27	49.05
Case of T_2 variation							
ΔT_2	-70%	-30%	-10%	0%	10%	50%	70%
ΔISE (%)	-16.25	-2.67	-0.83	0	0.83	7.98	18.4

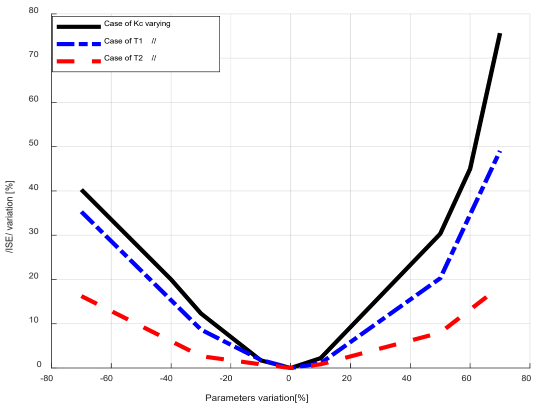

Figure 5. Speed ISE sensitivity to the PSS parameters variation around their optimal values

Note that the two parameters (K_C and T_1) variation of 50% gives a change of the speed ISE more than 15 %. On the other hand, the same change of T_2 gives an ISE change less than 8 %. The changing performance index curves show that the speed ISE is more sensitive to the two parameters K_C and T_1 (see Figure 5).

B. Increment Coefficients Adjustment

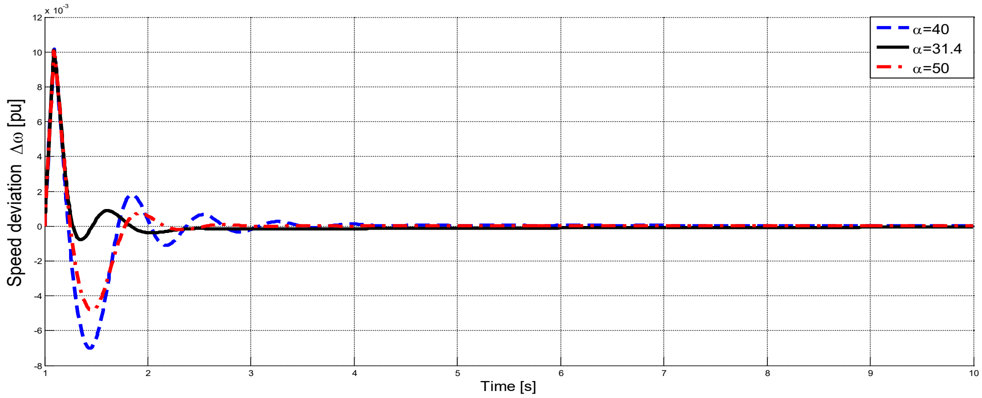

a. Tuning of the increment coefficient α

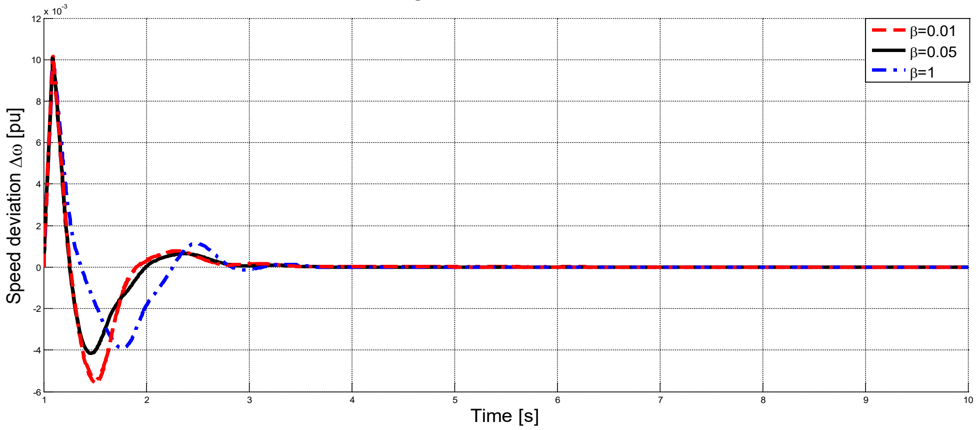

b. Tuning of the increment coefficient β

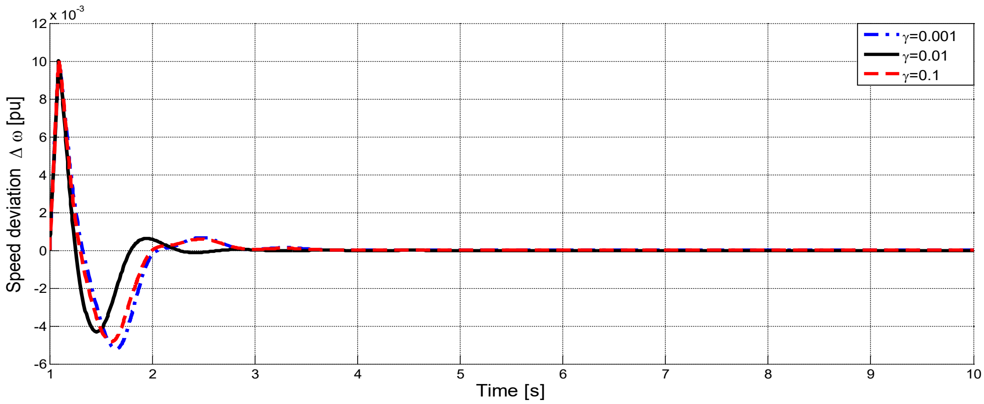

c. Tuning of the increment coefficient γ

Figure 6. Speed deviation dynamics for different increment coefficients (α, β and γ)

To update the PSS parameters online (K_c, T_1 or T_2) the equations (7, 8 and 9) are used. Initially, these parameters are set to their optimal values given by the genetic algorithm. Moreover, their upper and lower limits are chosen (after several simulation tests) around the optimal values, to determine each parameter range as follows:

$K_{c0} = K_c^{'} = 40$, $K_{c\min} = 20$ and $K_{c\max} = 70$, $T_{10} = T_1^{'} = 0.2$ s, $T_{1\min} = 0.025$ s and $T_{1\max} = 0.3$ s, $T_{20} = T_2^{'} = 0.078$ s, $T_{2\min} = 0.05$ s and $T_{2\max} = 0.09$ s.

The limits choice of each parameter is critical; the test of the system stability can be used to determine these limits.

Several simulation tests have been performed and used to adjust the values (α, β and γ). Some cases are presented in Figure 6 to justify the choice of these coefficients best values. In this case, the nominal operating point of the SMIBS has been considered, see Table 2.

Table 2. Operating points and loading conditions of the studied SMIBS [26], [37-38]

		Generator	*Load*		
Bus	*V*(pu)	*P* (pu)	*P'*(pu)	*Q'* (pu)	
1	1.00	1.00	0	0	Light
2	0.95	0.10	0	0	
3	1.00	1.00	0.055	-0.027	
1	1.00	1.00	0	0	Nominal
2	1.0007	0.90	0	0	
3	1.00	1.00	0.5	0.3	
1	1.00	1.00	0	0	Heavy
2	1.00	1.30	0	0	
3	1.00	1.00	0.72	-0.55	

Note that, by increasing "α", there is a good improvement in the performance index (ISE) but beyond the optimum value (α=31.4) this index begins to downgrade. In the same way, it is found that the best values of β and γ are 0.05 and 0.01 respectively.

The following Table summarizes the index performance (speed ISE) for different STPSSs:

Table 3. Performance index of different PSSs

Type of PSS	K_c	T_1	T_2	ISE$\times 10^{+3}$
CPSS	Fixed	Fixed	Fixed	8.110
STPSS1	Variable	Fixed	Fixed	1.842
STPSS2	Fixed	Variable	Fixed	2.636
STPSS3	Fixed	Fixed	Variable	2.820

For these simulation results, one can conclude that the K_c tuning is the best choice.

7. Performance and Robustness of the Proposed Controller

A. Case of a mono-machine system

Let us now present and compare the simulation results of the SMIBS in the case of the optimized fixed parameters PSS (GAPSS) and (STPSSs) for the different three loads. Remember that the GAPSS parameters have been carried out based on eigenvalues analysis as it has been mentioned previously.

To test the performance of the suggested controller and as well as its robustness, a large disturbance based on a three-phase short-circuits is applied in the same way of section (4.1). The obtained results are presented hereafter.

- *Performance of the STPSS*

The simulation results of the three STPSSs and the GAPSS, obtained in the case of the nominal load operating point are presented in figure 7.

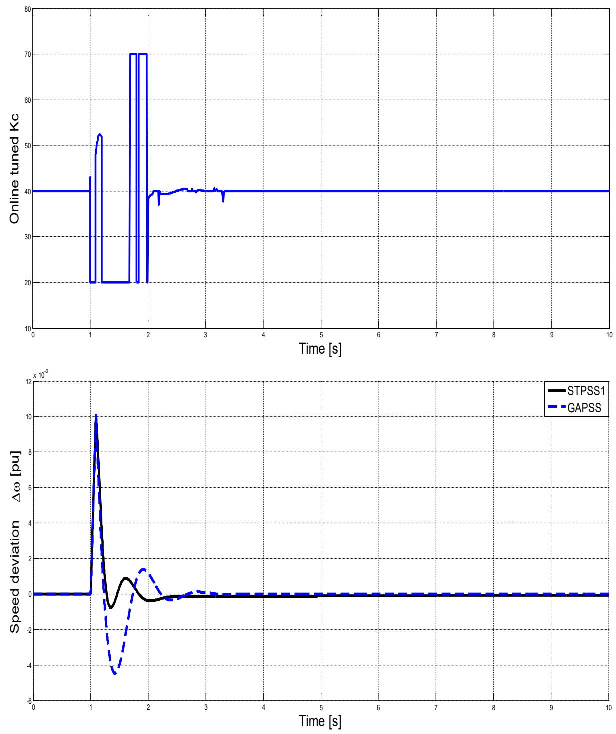

a. Case of an online tuning of K_c

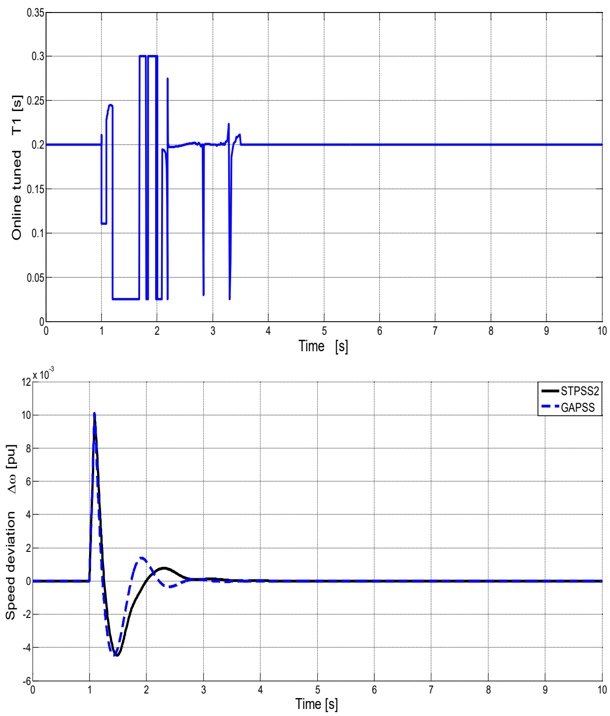

b- Case of an online tuning of T_1

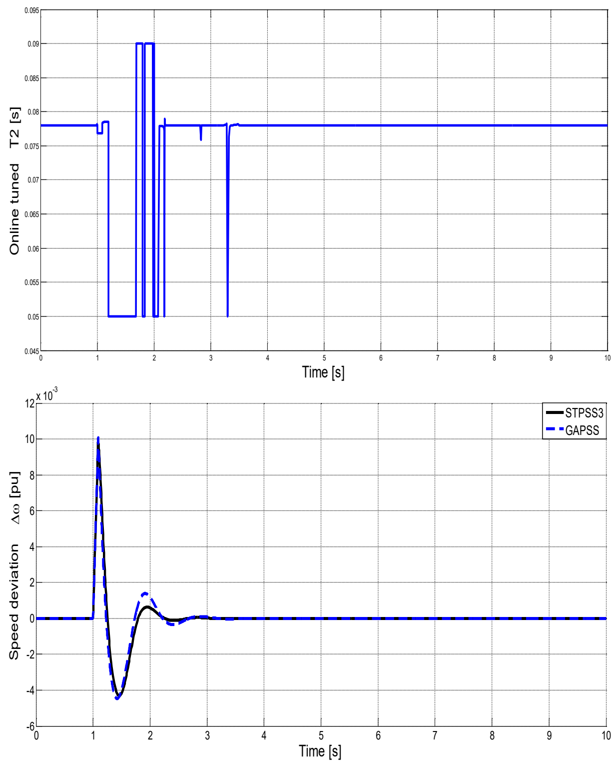

c- Case of an online tuning of T_2

Figure 7. Simulation results, a comparison between the STPSSs and the GAPSS performance

Table 4 presents in details the obtained results. It is clearly observed that the peak-to-peak amplitude is better in the case of K_c tuning (STPSS1). On the other hand, it is noted that the first peak remains practically the same regardless of the used PSS, since initially all PSSs have the same parameters. In addition, the settling time is improved by the STPSS1 from 3.38 s to 2.28 s relatively the case of the CPSS (32.45 %).

Moreover, the simulation results of Table 4 show clearly the good performance of the proposed PSS. In fact, one can note that the self-adjustment of each PSS parameter can improve the performance index of more than 65%.

Finally, it is concluded that once more the performance index enhancement is best in the case of the K_c adjustment (STPSS1), see Table 4.

Table 4. Performance comparison of different PSSs

Kind of PSS	1st peak	2nd peak	Peak to peak	ISE×10^3	ΔISE %
CPSS	0.01008	-0.00451	0.01459	8.110	0
STPSS1	0.01008	-0.00077	0.010852	1.842	77.28
STPSS2	0.01001	-0.00447	0.01448	2.636	67.50
STPSS3	0.01001	-0.00424	0.014246	2.820	65.23

- *Robustness of the STPSS against load variation*

To show the robustness of the proposed PSS, against the load variation, here are the simulation results corresponding to these three loads of Table 2 in the case of the STPSS1 and the GAPSS performed for the nominal loading condition.

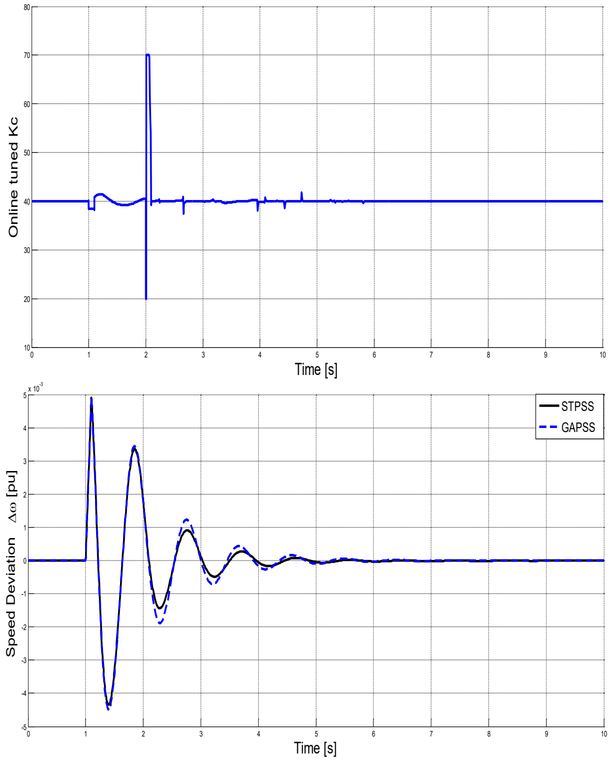

a. Light Loading Condition

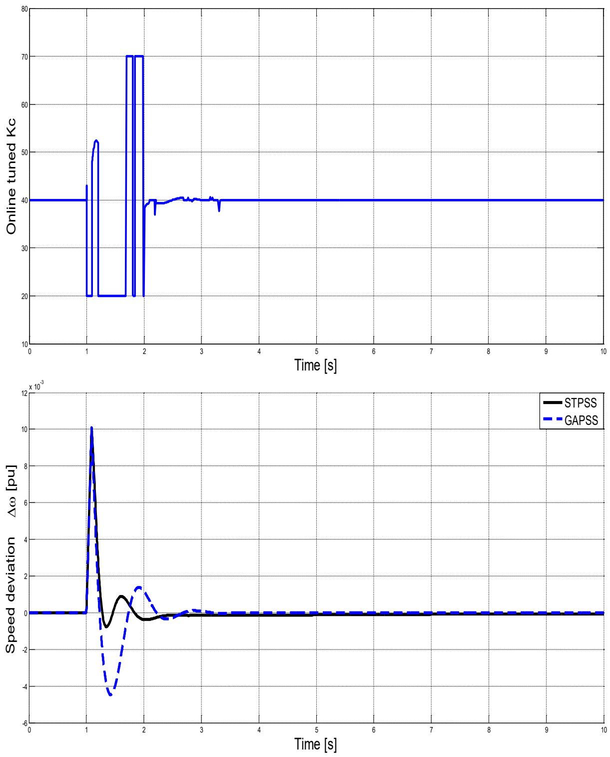

b. Nominal Loading Condition

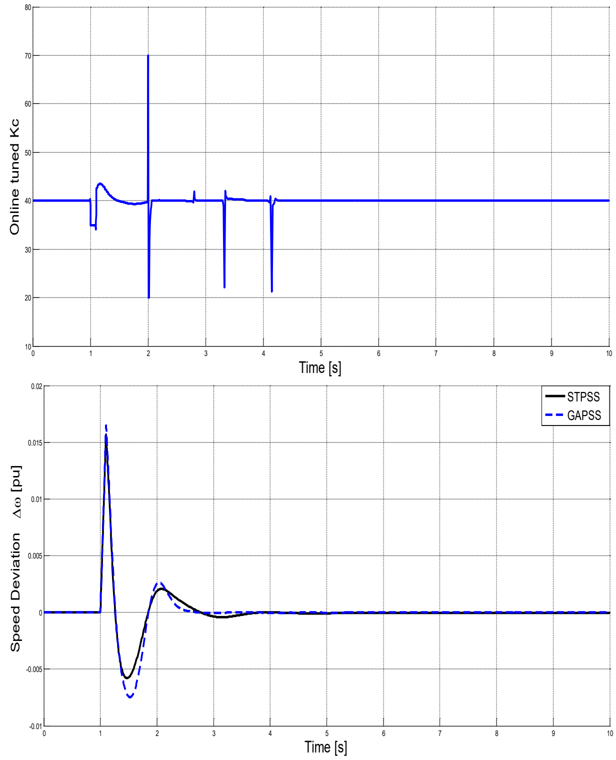

c. Heavy Loading Condition

Figure 8. Speed deviation and K_c versus time for different loading conditions

Table 5. Performance comparison of PSSs for different loading conditions

Load	Kind of PSS	1st peak $\times 10^{+3}$	2nd peak $\times 10^{+3}$	Peak to peak $\times 10^{+3}$	ISE$\times 10^3$	ΔISE %
Light	CPSS	4.952	-4.477	9.429	3.1983	7.10
	STPSS1	4.372	-4.276	8.648	2.9715	
Nominal	CPSS	10.08	-4.510	14.590	8.1100	77.28
	STPSS1	10.08	-0.770	10.852	1.8420	
Heavy	CPSS	16.460	-7.471	23.931	2.5807	3.10
	STPSS1	15.660	-5.787	21.447	2.5010	

From these results obtained for different loading conditions, one can notice that the low loaded system is less amortized and represented the most critical operating point. In fact, it is found, in this case, that the gain K_c is auto-adjusted until 4.5 seconds.

In general, it is clear that the proposed STPSS is more robust than the GAPSS against load variation, see figure 8 and Table 5 that shows the superiority of the proposed PSS over the conventional PSS in terms of the speed deviation peaks and the index performance value.

B. Case of a Two-Area Multimachine system

- Description of a Two-Area Multimachine Power System

In order to apply the proposed method to a multimachine system, we chose a system that was first described in [39].This system presents different oscillation modes (inter area as well as local modes). It consists of two regions connected across a 220 km line. Both two areas are symmetrical and each has two generators. All generators have the same parameters. The system data are presented in and Figure 9 shows its one-line diagram [39].

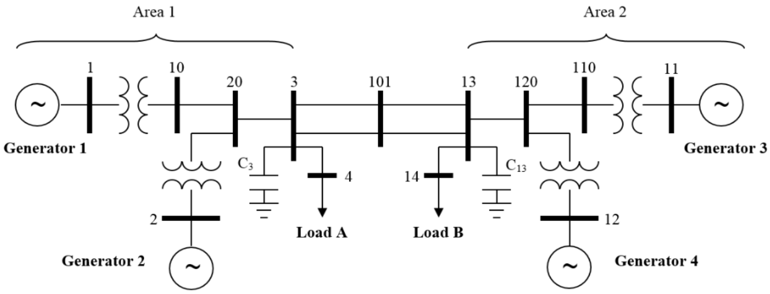

Figure 9. Two-area four machines test system

- *Implementation Details and Case Study*

To make a comparative study between the proposed STPSS and the optimized PSS, the PSSs parameters presented in the reference [40] have been chosen. In this work, the PSSs parameters have been optimized by genetic algorithm using an objective function in order to minimize the vector of damping coefficients.

In this study, a power flow of 400 MW from area 1 to area 2 has been considered for two different configurations:

- Configuration 1 with two lines between bus 3 and 101
- Configuration 2 with a single line between bus 3 and 101

Dealing with these two different configurations of the power system, instead of the operating points, is due to the fact that the PSS must also be able to stabilize the system even if it changes configuration (loss of a line for example).

To disrupt the network, the same scenario taken into account in [40] has been simulated, which consists of a three-phase short-circuit fault near bus 3 on the 3-101 line that occurred at the moment t = 0.1s. Then the line is open at t = 0.19s, the fault disappears and it (the line) is closed at t=0.20s. Table 6 shows participation factors and frequencies of each generator for different electromechanical oscillatory modes and for both configurations.

The second configuration is a typical example of inter-area oscillations. One can notice that the mode (0.183 ± 5.999i) is dominant for the generators G_1 and G_2, while the mode (-0.188 ± 5.987i) is dominant for the generators G_3 and G_4. These two modes correspond to local modes and characterize the interaction between the two generators of the same area. On the other hand, the mode (0.046 ± 2.901i) corresponds to an inter-area mode and characterizes the interaction between generators of one region (G_1 and G_2 for example) and the generators of the other area (G_3 and G_4).

Table 6. Participation Factors of different electromechanical modes

Configuration	Modes	G_1	G_2	G_3	G_4	Frequency (Hz)
1	0.068 ± 3.713i	0.2414	0.1296	0.3381	0.2869	0.5910
	-0.217 ± 5.989i	0.2248	0.2613	0.3180	0.3271	0.9531
	-0.229 ± 6.016i	0.2753	0.3670	0.1992	0.2899	0.9576
2	-0.183 ± 5.999i	0.5095	0.5945	0.1526	0.1881	0.4618
	-0.188 ± 5.987i	0.1592	0.1803	0.5363	0.5701	0.9547
	0.046 ± 2.901i	0.1413	0.0738	0.4095	0.3835	0.9529

- *Implementation of STPSS*

To perform a comparative study, the same PSSs parameters of [40] placed on the two generators (G_2 of first area and G_3 of second area) have been adopted as has been mentioned previously. These parameters of the two lead-lag PSSs are summarized in the following table:

Table 7. PSSs parameters of [40]

	Bus	$K_{C0}(i)$	Tw (s)	T_1=T_3 (s)	T_2=T_4 (s)
PSS(i=2)	2	47.16	20	0.7109	0.15500
PSS(i=3)	11	300.0		0.1500	0.08431

Table 8. Simulation results

	α_1	α_2	K_{c02}	K_{C03}	ISE1	ISE2	ISE3	ISE4	∑ISE$_i$	
Case of [40]	0	0	47.16	300	13.10	4.00	16.36	21.22	54.67	Configuration 1 Two lines between bus 3 and 101
Control strategy 1	74.5797	674.145			12.58	3.81	15.30	21.20	52.89	
Control strategy 2	-97.663	-67.205			8.59	3.60	8.10	15.12	35.41	
Improvement by control strategy 1					3.93%	4.79%	6.47%	0.09%	3.26%	
Improvement by control strategy 2					34.34%	9.93%	50.50%	28.73%	33.05%	
Case of [40]	0	0	47.16	300	9.74	4.93	25.36	24.08	64.11	Configuration 2 One line between bus 3 and 101
Control strategy 1	74.5797	674.145			9.22	4.63	23.08	22.93	59.86	
Control strategy 2	-97.663	-67.205			8.05	4.02	20.42	20.47	52.95	
Improvement by control strategy 1					5.40%	6.01%	9.00%	4.75%	6.63%	
Improvement by control strategy 2					17.39%	18.34%	19.50%	15.00%	17.40%	

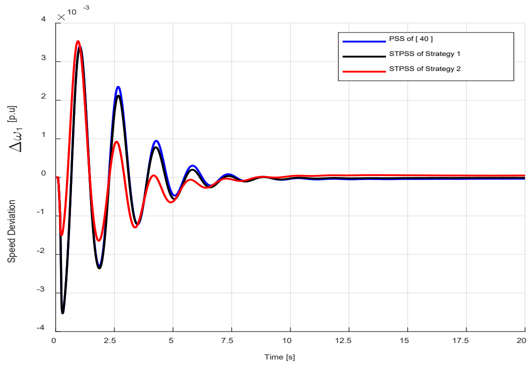

a. Configuration 1

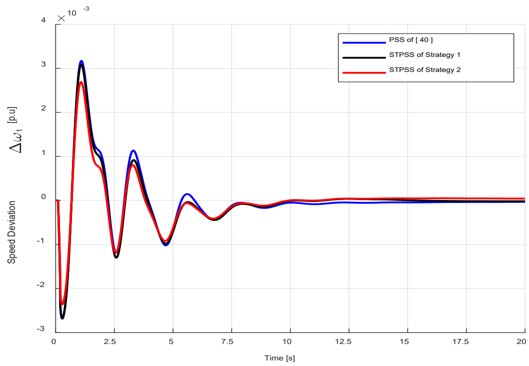

b. Configuration 2

Figure 10. Comparison between speed deviations of Generator 1 for two configurations

Let us now present the self-tuning procedure used in this case of multimachine inter-area system. For this purpose, two strategies have been carried out:

a. The first strategy uses directly “(7)” i.e. it assumes that each generator self-adjusts its PSS parameters independently.
b. The second strategy takes into account the interaction between the two zones of the system and considers that the tuned parameters of different PSSs are interdependent. In this case, the following equation is proposed for self-tuning of PSS gain:

$$K_{Cj}(k+1)=K_{C0j}(k)-\sum_{i=1}^{n}\alpha_i\left(\frac{\partial(\Delta\omega_i)}{dK_{Ci}}\right) \tag{11}$$

Where:
i,j: are indexes of the PSS index
n: is the number of installed PSSs.

To determine the coefficients α_i, the PO method is used. Table 8 summarizes all results obtained from the self-adjustment coefficients and the ISEs of each generator and each variant for both configurations.

The dynamic response of the four generators as well as the variation of the gain are given by figures 10, 11, 12 and 13 for both configurations.

In the case of the 1st configuration (Figure10-a), it is clear that the two STPSSs have significantly minimized the ISE, especially when the second control strategy is used. In fact, the performance enhancement (relatively to the GAPSS) is about 33% (case of the 2nd strategy) on the other hand, it is about 3.2% (case of 1st strategy).

Elsewhere, in the case of the 2nd configuration (see Figure10-b), the performance enhancement is about 17.4% (case of the 2nd strategy). On the other hand, it is about 6.6% (case of 1st strategy).

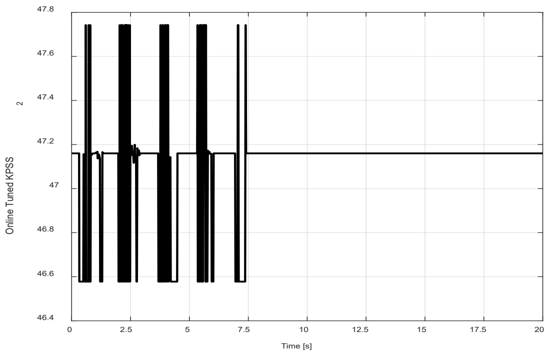

a. Case of control strategy 1 and configuration 1

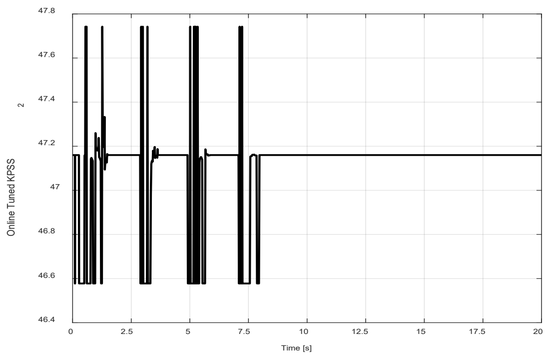

b. Case of control strategy 1 and configuration 2

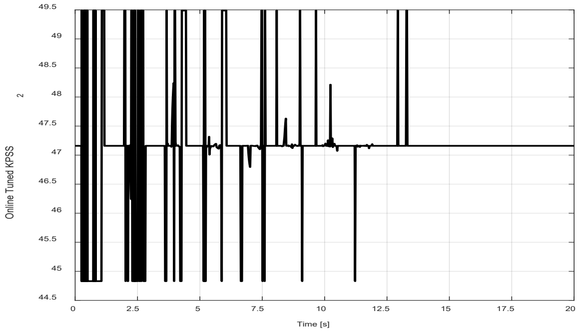

c. Case of control strategy 2 and configuration 1

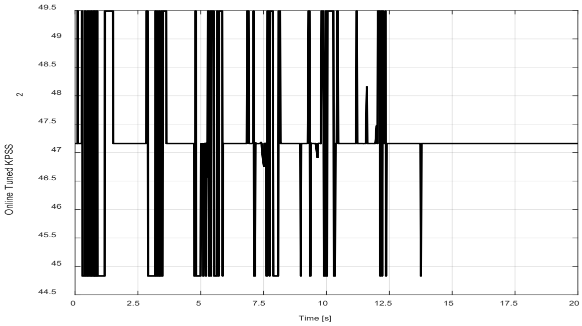

d. Case of control strategy 2 and configuration 2

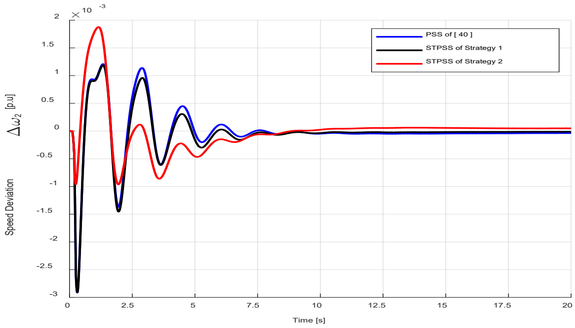

e- Speed deviation of generator 2 and configuration 1

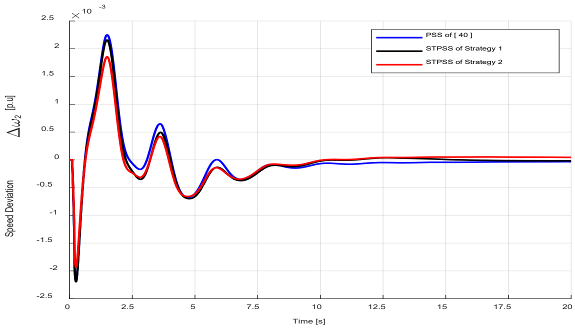

f- Speed deviation of generator 2 and configuration 2

Figure 11. Speed deviation of generator 2 and its PSS gain for different control strategies and system configurations

Note that generator G_2 is equipped with a PSS and it has the largest participation factor in the case of local mode of area 1. It is observed also that the 1st configuration presents always the highest performance when the second control strategy is used, except the lowest improvement of its ISE comparatively to the ISEs of the other generators. In the case of the second configuration, the increase of the performance is about 18.34%. While it is noted that the variations of the gains depends on the changes in the speed deviation. It is also noticed that the gain becomes constant in the steady state (in about 8 seconds, for the first control strategy, and 14 s in the second strategy). This means that even if the speed deviation of the concerned generator stabilizes, it remains in action until the other generators stabilize.

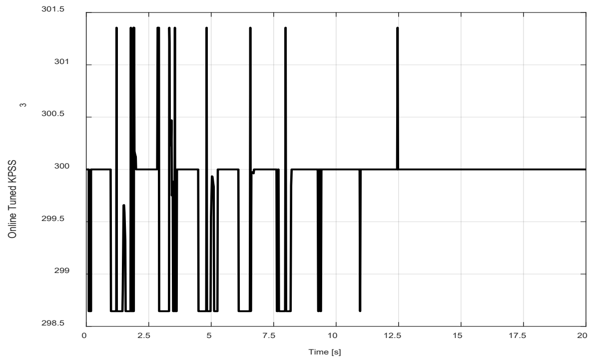

a. Case of control strategy 1 and configuration 1

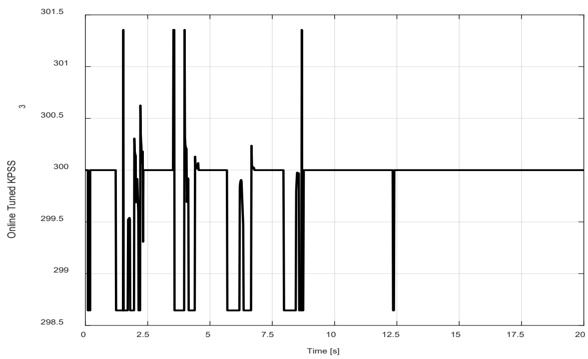

b. Case of control strategy 1 and configuration 2

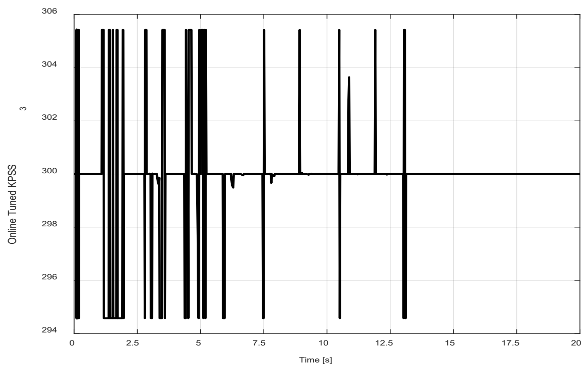

c. Case of control strategy 2 and configuration 1

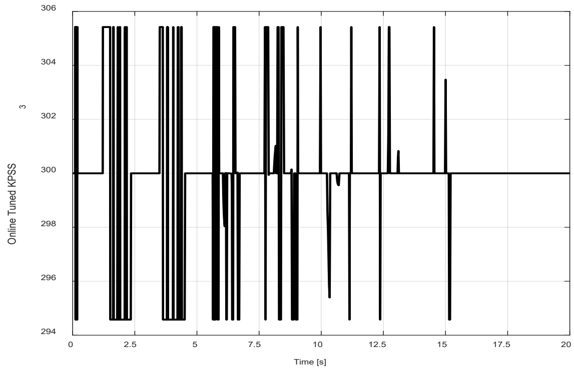

d. Case of control strategy 2 and configuration 2

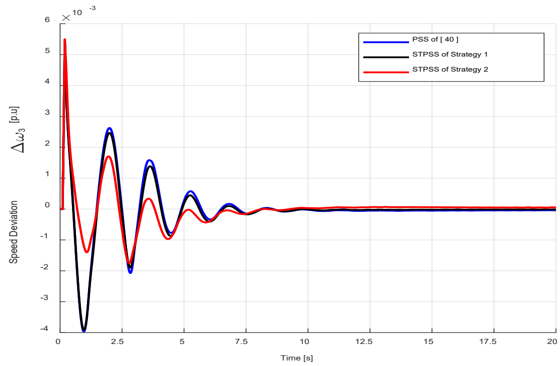

e- Speed deviation of generator 3 and configuration 1

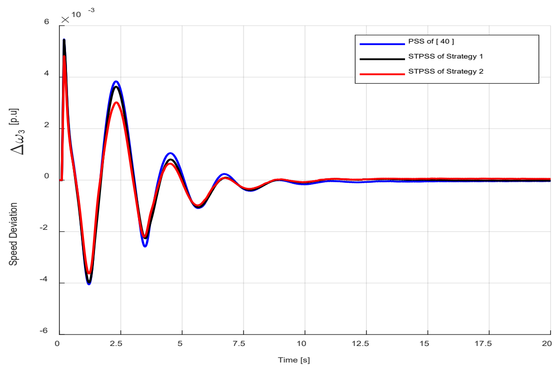

f- Speed deviation of generator 3 and configuration 1

Figure 12- Speed deviation of generator 3 and its PSS gain for different control strategies and system configurations

Elsewhere, generator 3 of figure 12 presents the highest inter-area participation factor. It is found that when the STPSS auto-adjusted by strategy 2, the performance improvement has reached 50% comparatively to strategy 1 where the PSSs are assumed to operate independently. In fact, in this latter case, the performance increasing is about only at 6%. In addition, this improvement drops to about a half when the configuration changes (addition of a line loss). Despite this, it is found that the performance of STPSS auto-adjusted by strategy 1 has increased from 6.47% to 9%. This can be explained by the fact that the PSS auto-adjusted by the 1st strategy stabilizes only the local modes. However, the PSS auto-adjusted by strategy

2 stabilizes all the modes (local and inter-area modes). As mentioned previously, the same reproaches already pointed out concerning the variation in gains accompany the variation of speed deviation. It is also noticed that the gain stabilizes in about 12.5 seconds in the case of the 1st control strategy. In another way, its variation persists until the whole system stabilizes, in the case of the second strategy.

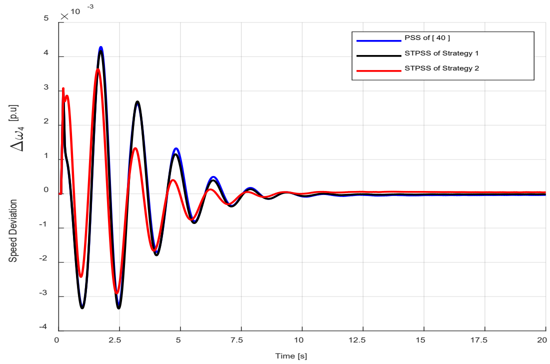

a. Configuration 1: Two lines between bus 3-101

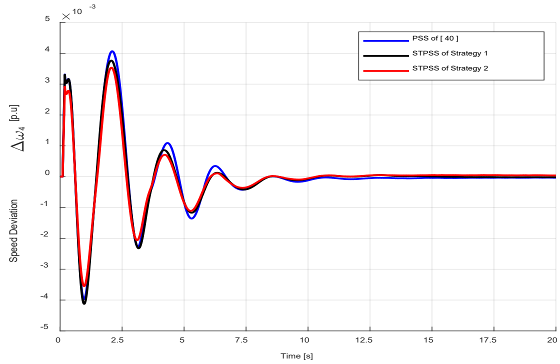

b. Configuration 2: One line between bus 3 and 101

Figure 13. Comparison between speed deviations of generator 4

As far as generator 4 is concerned for configuration 1, the STPSS (tuned by strategy 1) operation remains almost identical to that of the basic PSS [40] optimized by the genetic algorithm. The same remarks will remain valid regarding configuration 1 and 2. The STPSS in strategy 1 is indeed the most competitive.

Generally, it is observed that the second strategy, assuming interdependent PSSs parameters, is better and more adapted to well-damp inter-area rotoric oscillations. However, for local modes, it is enough to use the first strategy to self-tune STPSSs parameters. In contrast, STPSS always gives better results than the GAPSS that proves the superiority of the proposed self-adjustment method.

8. Conclusion

In this paper, a robust and adaptive new PSS design (based on a self-setting of its settings) was presented. The parameters of a SMIBS PSS and a typical inter-area multimachine system are set online based on the speed gradient. Simulation results of the system's dynamic response subject to a three-phase fault perturbation for different loading conditions. It is presented and discussed in the case of a single-machine system. Whereas for the study of a multimachine system, two strategies have been proposed to self-tune the PSSs parameters for two different configurations of the studied power system. Simulation results have been presented also and shown the effectiveness of the proposed self-tuned controller. In fact, a comparison study between STPSS and GAPSS performance has been made and thus showed the superiority of the proposed design approach in terms of speed oscillations damping and robustness against load variation, especially in the case of the amplifier gain online self-adjustment.

APPENDIX A

Table 9. Nomenclature

Symbol	Meaning	Symbol	Meaning
r	Disturbance matrix	U	Control Vector
A	State matrix	H	Inertia constant in (seconds)
B	Command matrix	D	Damping constant
P	Disturbance vector	ω_0	Synchronous angular velocity
δ	Rotor angle	ω	Angular velocity of generator
E'_q	q-axis component of the transient electromagnetic field proportional to the field winding flux linkages	E_{fd}	Equivalent excitation voltage (Field circuit voltage)
f	Frequency	K_a	AVR gain
T_a	AVR time constant	T'_{d0}	Time constant of excitation circuit

Table 10. Power system data [38]

Line Data	R_1 (p.u)	X_1 (p.u)	R_2 (p.u)	X_2 (p.u)	b (p.u)
	0.012	0.3	0.012	0.3	0.066
Generator Data	X_d (p.u)	X'_d (p.u)	X_q (p.u)	T'_{do} (Sec.)	
	1.720	0.450	0.450	6.300	
	H (Sec.)	f (Hz)	K_a	T_a (Sec.)	
	4.00	60	20	0.03	

9. References

[1]. Hooshmand R, Ataei M. “An Auto-Tuning Fuzzy Logic PSS Design under Multi-operating Conditions Using Real-Coded Genetic Algorithm,” *Journal of Electrical Systems 2009*; 5:1-3.

[2]. Ataei M, Hooshmand R, Moein P. “A Wide Range Robust PSS Design Based on Power System Pole-Placement Using Linear Matrix Inequality,” *Journal of Electrical Engineering*, 2012; 4:233–241.

[3]. Ganjefar S, Alizadeh M. “A novel adaptive power system stabilizer design using the self-recurrent wavelet neural networks via adaptive learning rates,” *International Transactions on Electrical Energy Systems*, 2012, DOI: 10.1002/etep.1616.

[4]. Ziqian L. “Modeling and Simulation of Self-Tuning PI Control for Electrical Machines,” *Asian Power Electronics Journal*, 2007; 1:58-62.

[5]. Malikov A, AI M. “Effect of Power System Stabilizers and Automatic Voltage Regulator Gain on Synchronizing and Damping Torques,” ZONT, 2009; 1: 93-102.

[6]. DeMello F, Concordia C. “Concepts of Synchronous Machines Stability as Affected by Excitation Control,” *IEEE Transactions*, 1969; 4:316-329.

[7]. Adrian A. On Power System Stabilizers: Genetic Algorithm Based Tuning and Economic Worth as Incillary Services, Thesis for the Degree of Doctor Philosophy, Göteborg, Sweden, 2004.

[8]. Kundur P, Paserba J, Ajjarapu V, Andersson G, Bose A, Canizares C, Hatziargyriou N, Hill D, Stankovic A, Taylor C, Cutsem T. V and Vittal V. “Definition and Classification

of Power System Stability," *IEEE Transaction on Power Systems of Power System Stability 2004*; 19: 1387 - 1401.

[9]. Shahgholian G, Faiz J. "The Effect of Power System Stabilizer on Small Signal Stability in Single Machine Infinite Bus," *International Journal of Electrical and Power Engineering 2010*; 4:45-53.

[10]. Shahgholian G. "Review of Power System Stabilizer: Application, Modeling, Analysis and Control Strategy," *International Journal on Technical and Physical Problems of Engineering 2013*; 41-52.

[11]. Chédot L and Friedrich G. "Comparisons of Direct and Adaptative Optimal Controls for Interior Permanent Magnet Synchronous Integrated Starter Generator," *Electric Machines and Drives Conference*, IEMDC'03. Madison, WI, USA 2003; 1: 183 - 187.

[12]. C. Lim and T. Hiyama, "Self-tuning Control Scheme for Stability Enhancement of Multimachine Power Systems," *IEE Proceedings of C-Generation, Transmission and Distribution*, vol. 137, pp. 269-275, 1990. DOI: 10.1049/ip-c.1990.0036

[13]. R. Doraiswami and W. Liu, "Real-time Estimation of the Parameters of Power System Small Signal Oscillations," *IEEE Transactions on Power Systems*, vol. 8, pp. 74-83, 1993.

[14]. G.-P. Chen, O. Malik, G. Hope, Y.-H. Qin and G.-Y. Xu, "An Adaptive Power System Stabilizer Based on the Self-Optimizing Pole Shifting Control Strategy," *IEEE Transactions on Energy Conversion*, vol. 8, pp. 639-645, 1993.

[15]. H. Seifi, "On-Line Adaptive Stabilization of a Turbo-Generator," *Computers & Electrical Engineering*, vol. 21, pp. 57-68, 1995.

[16]. M. Abido and Y. Abdel-Magid, "Adaptive Tuning of Power System Stabilizers Using Radial Basis Function Networks," *Electric Power Systems Research*, vol. 49, pp. 21-29, 1999.

[17]. R. Segal, A. Sharma, and M. Kothari, "A Self-Tuning Power System Stabilizer Based on Artificial Neural Network," *International Journal of Electrical Power & Energy Systems*, vol. 26, pp. 423-430, 2004.

[18]. G. Ramakrishna and O. Malik, "Adaptive PSS Using a Simple On-Line Identifier and Linear Pole-Shift Controller," *Electric Power Systems Research*, vol. 80, pp. 406-416, 2010.

[19]. E. Nechadi, "Commande et Stabilite d'un Système Electro-Energétique," Thèse de Doctorat, Université d'Oum El Bouaghi, Algerie, 2013.

[20]. A.A. Ba-Muqabel, M.A. Abido. "Review of Conventional Power System Stabilizer Design Methods," *IEEE/GCC*, pp. 1-7, Manama, March 2006.

[21]. Urdaneta, A. J., Bacalao, N. J., Feijoo, B., et al. "Tuning of power system stabilizers using optimization techniques," *IEEE Transactions on Power Systems*, 1991, vol. 6, no 2, p. 127-134.

[22]. Sharaf, A.M. & Lie, Tek Tjing & Gooi, H.B. "Neural Network Based Power System Stabilizers,". 306 - 309. 10.1109/ANNES.1993.323018 (1993).

[23]. M. Tofighi, M. Alizadeh, S. Ganjefar, M. Alizadeh. "Direct adaptive power system stabilizer design using fuzzy wavelet neural network with self-recurrent consequent part," Appl Soft Comput, 28 (2015), pp. 514-526

[24]. Jesús Fraile-Ardanuy, P.J. Zufiria, "Design and comparison of adaptive power system stabilizers based on neural fuzzy networks and genetic algorithms," Neurocomputing, Volume 70, Issues16–18, 2007, Pages 2902-2912, https:// doi.org /10.1016 /j.neucom .2006 .06.014 .

[25]. Kumar J, Kumar P, Mahesh A and Shrivastava "A. Power System Stabilizer Based On Artificial Neural Network, Power and Energy Systems," *International Conference – IEEE* 2011; 1-6.

[26]. Rusejla S. "Single Machine Infinite Bus System," Internal report Zurich 2003.

[27]. Jhamad M, Surbhi S. "A Novel PSS Design for Single Machine Infinite Bus System Based on Artificial Bee Colony," *International Journal of Scientific Research Engineering & Technology (IJSRET)* 2013, 2: 532-537.

[28]. Mahdiyeh E, Hussain S and Azah M. “Application of Artificial Intelligent Techniques in PSS Design, A Survey of the State-of-the-Art Methods,” Przegląd Elektrotechniczny. 2011; 87:188 - 197.

[29]. Mekhanet M, Mokrani L and Choucha A. “Adaptive Neuro-Genetic Based Power System Stabilizer Design,” *Journal of Electrical and Control Engineering* 2012; 2:7-12.

[30]. Abido M, Abdel-Magid Y. A Hybrid Neuro-fuzzy Power System Stabilizer for Multimachine Power Systems. *Power Systems, IEEE Transactions* 1998; 13, 1323 - 1330.

[31]. Jalilvand A, Keshavarzi M and Khatibi M. “Optimal tuning of PSS parameters for damping improvement using PSO algorithm,” *Conference (PEOCO) IEEE Shah Alam* 2010: 1-6.

[32]. WenxinL,GaneshK. Venayagamoorthy, Donald C. Wunsch II, “Adaptive Neural Network Based Power System Stabilizer, Neural Networks,” *Elsevier Science 2003, Special issue*, 891–898.

[33]. Linda M, Nair D. “Optimal Design of Fuzzy Based Power System Stabilizer Self Tuned by Robust Search Algorithm,” *Journal of Computing* 2009; 1: 44 - 48.

[34]. Shoaib Shahriar M, Ashik M, Shahid U. “Design and Analysis of a Model Predictive Unified Power Flow Controller (MPUPFC) for Power System Stability Assessment,” *International Journal of Electrical & Computer Sciences 2008*; 12, 32 - 37.

[35]. Shayeghi H, Safari A, Shayanfar H. “Multimachine Power System Stabilizers Design Using PSO Algorithm,” *World Academy of Science, Engineering and Technology 2008*; 2: 713 - 720.

[36]. Kushwaha M, Khare R. “Dynamic Stability Enhancement of Power System Using Fuzzy Logic Based Power System Stabilizer,” *In IEEE Power, Energy and Control, International Conference (ICPEC) 2013*; 213- 219.

[37]. M. Mekhanet, L. Mokrani, A. Ameur, and Y. Attia, “Adaptive fuzzy gain of power system stabilizer to improve the global stability,” *Bulletin of Electrical Engineering and Informatics (BEEI)*, vol. 5, pp. 421-429, 2016.

[38]. R.K. Ranjan, “Parametric Approach to Steady-State Stability Analysis of Power Systems,” Master’s Thesis, Graduate College of the University of Illionois at Urbana-Champion, 1992.

[39]. M. Klein, G. J. Rogers and P. Kundur, “A fundamental study of inter-area oscillations in power systems,” in *IEEE Transactions on Power Systems*, vol. 6, no. 3, pp. 914-921, Aug. 1991.

[40]. A. Hasanovic and A. Feliachi, “Genetic algorithm based inter-area oscillation damping controller design using MATLAB,” *IEEE Power Engineering Society Summer Meeting*, Chicago, IL, USA, 2002, pp. 1136-1141 vol.3.

Mohammed MEKHANET was born in Laghouat, Algeria, in 1961. He obtained his Electrical Engineering diploma in 1987, at Polytechnic National School of Algiers, Algeria, and his *Magister* and *PhD degrees* in 2007 and 2018 respectively. In 2007, he joined the electrical Engineering Department of Laghouat University, as Assistant Lecturer.
He is also a Team Member of "Power System Optimization and Control" research group of LACoSERE Laboratory, Laghouat University. His Main research interests include Optimization and CAD in Electric power System, Power system stabilizer.
Correspondence Address: LACoSERE Laboratory, Electrical Engineering Department University Amar Telidji-Laghouat BP 37G Lagouat, Algeria.

Lakhdar MOKRANI was born in Batna (Algeria), on March 5, 1970. He obtained his *engin*eer and *Ph.D*. degrees in electrical engineering, in 1994, 2005 respectively from Batna University (Algeria). In 1997, he joined the electrical engineering department of Laghouat University (Algeria) as Assistant Lecturer From 2005 to 2012, he was a Lecturer, and since 2012, he is a *full professor* at the same department. He is also the responsible of "Control and Energy Management of Electrical Systems" research group of the LACoSERE Laboratory, Laghouat University (Algeria).
His main research area includes Modelling and CAD of Electrical Machines, Electrical Drives Control and Renewable Energy Systems Control and Management.
Correspondence address: LACoSERE Laboratory, Electrical Engineering Department Amar Telidji University of Laghouat, Algeria.